

Content from this work may be used under the terms of the CC BY 3.0 licence (© 2018). Any distribution of this work must maintain attribution to the author(s), title of the work, publisher, and DOI.

CONCEPTUAL DESIGN FOR SLS 2.0

M. Dehler, A. Streun, A. Citterio, T. Garvey, M. Hahn, L. Schulz, M. Negrazus, V. Vranković
 PSI, Villigen PSI, Switzerland

Abstract

After 17 years of user operation, we plan to do an upgrade of the Swiss Light Source (SLS) in the period 2023-2024. The entire storage ring will be replaced by a new layout allowing operation at emittances lowered by factors of 40-50. This is made possible by small aperture magnets allowing for a multi bend achromat design and - a special feature for SLS 2.0 - with reverse bends combined with longitudinal gradient bends (LGB) leading to zero dispersion at the maximum magnetic field, thus minimizing the quantum excitation of the beam due to synchrotron radiation. The compact magnet layout makes use of offset quadrupoles, combined function magnets and longitudinal gradient bends. All vacuum chambers along the electron beam path will be coated with a non-evaporable getter (NEG) film to ensure low photo-desorption and a quick vacuum conditioning. Numerical simulations of instability thresholds have been performed. We expect values on the order of 2 mA for the single bunch current.

INTRODUCTION

Table 1: Main Parameters Of SLS 2.0 Compared To SLS

	SLS 2.0	SLS
Circumference [m]	290.4	288.0
Energy [GeV]	2.4	2.4
Current [mA]	400	400
Main RF frequency [MHz]	499.6	499.6
Nominal RF voltage [kV]	1420	2080
Harmonic number	484	480
Filling pattern gap	10%	19%
Damping times $\tau_{x,y,E}$ [ms]	4.9/8.4/6.5	8.6/8.6/4.3

The SLS started user operation in 2001 and has been operated in top-up mode since then. Today it is fully equipped with a set of 18 beam lines delivering about 5000 hours of user time per year with an excellent availability.

While it was state of the art at the time, a new generation of light sources are coming into operation or development, which make use of features such as advanced optics using low aperture magnets resulting in a dramatically reduced emittance. Given that the improved machine layout still needs to fit the existing facility with minimum changes, scaling existing designs, as e.g. for MAX-IV, would not have led to the required improvement in emittance of at least 30. A novel type of lattice was developed, which makes use of longitudinal gradient bends and reverse bends. At the price of stronger than anticipated modifications in the shielding walls and shifts in the source points of several beam lines, the old design with a three fold symmetry and three differ-

ent types of straights will be replaced by a strictly regular layout with twelve fold symmetry.

The low vacuum chamber aperture of 20 mm diameter used in the design poses challenges from two sides. Vacuum conductance along the chamber (worse by more than a factor five in comparison to SLS) becomes negligible, so that distributed pumping becomes essential. Also resistive effects leading e.g. to microwave instabilities need to be investigated closely. A comparison of the main parameters of the upgrade with the original SLS is shown in Table 1.

OPTICS

The zero-current horizontal emittance in a storage ring is determined by the equilibrium between radiation damping and quantum excitation. The latter depends on the rate of photon emission, which is given by the strength of the magnetic field, and on the local dispersion function, because after emission of a photon, an electron starts an oscillation around the closed orbit corresponding to its reduced energy. The damping of horizontal oscillations thus excited is given by the total radiated power, which depends on the magnetic field strength, and by the horizontal ‘share’ of the overall damping, which is affected by transverse gradients in combined-function bending magnets.

The quantum excitation can be minimized by the use of longitudinal-gradient bends (LGBs, bending magnets for which the field varies along the beam path), while suppressing the dispersion at the LGB center, where the field is strongest. In a conventional periodic cell, this would lead to an over-focusing of the transverse beta function β_x , since also the bending magnets have a defocusing effects on the dispersion. This can be solved by the use of small reverse bends (RBs), realized in the SLS 2.0 lattice by generating the reverse kicks by a transverse offset of the horizontal-focusing quadrupoles nearby.

A welcome effect of this strategy is the enhanced radiation damping. The field variation in the LGB increases the radiated power compared to classical homogeneous bending magnets. In addition, the reverse bends increase the total absolute bending angle to values larger than 360° . Altogether, a lattice cell combining LGBs and RBs can provide up to a five times lower equilibrium emittance compared to a conventional cell [1].

Figure 1 shows the fundamental building block of the lattice, a cell consisting of a center LGB with adjacent vertically focusing bends (VB) and two reverse bends. Five full and two half LGB-RB cells form one of the twelve identical 7-bend achromat arcs (7BAs) as shown in Fig. 2. Some cells will use LG-superbends of up to 6 Tesla peak-field [2] instead of the normal LGBs in order to provide x-rays in the 50 to 100-keV range. Table 2 compares the main parameters of

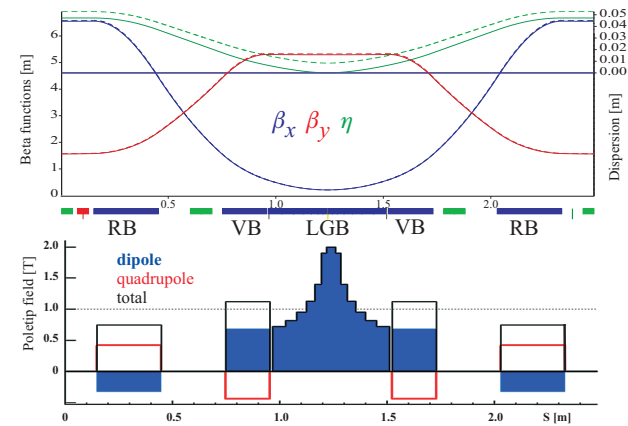


Figure 1: Optical functions and field components for the SLS 2.0 lattice cell containing a center LGB with adjacent vertically focusing bends (VB), and two RBs. If the RB were a pure quadrupole, the optical functions would follow the dashed lines in the upper plot and the emittance would be 4.5 time larger. The field components in the lower plot refer to the poletip field at 13 mm bore radius.

the upgraded lattice with the present SLS. An interesting property is the negative momentum compaction factor α as in proton synchrotrons below transition. Here the positive dependence between time-of-flight and momentum is over-compensated by the RBs.

All twelve straight sections are 5.5 m long. Eight full straights and three half straights are available for undulator installation, the others being required for injection elements and RF cavities. The higher lattice symmetry compared to SLS leads to modifications of the lattice footprint, mainly affecting the regions of the present longitudinal straights, while moderately affecting the others.

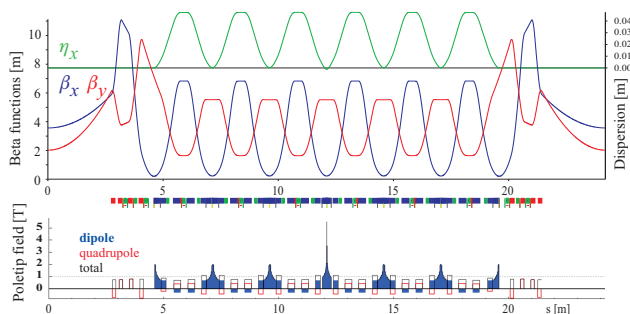


Figure 2: Optical functions and field components for one 7BA-arc where the center LGB has been interchanged by a super-LGB of 5.5 T peak field. Bending magnets are in dark blue, quadrupoles red and sextupoles green.

The lattice has a relative momentum acceptance of about 5% providing a Touschek-dominated beam lifetime of about 9 hours (similar to SLS now) and a horizontal dynamic aperture of about ± 6 mm at the point of injection. This allows off-axis injection, accumulation and top-up using the existing injector.

Table 2: Main parameters for the SLS 2.0 upgrade lattice including three superbends in comparison to the existing SLS lattice. The arrows (\rightarrow) indicates the increase due to intra-beam scattering at a nominal current of 400 mA in 400 of 484 bunches for 10 pm of vertical emittance and assume a third harmonic RF-system for bunch lengthening.

	SLS 2.0	SLS
Hor. damping partition J_x	1.71	1.00
Momentum compaction α [$\cdot 10^{-3}$]	-1.33	6.04
Total abs. bending angle	561.6°	374.7°
Lattice tunes $\nu_{x/y}$	39.2/15.3	20.4/8.7
Natural chromaticities $\xi_{x/y}$	-95/ -35	-67/ -21
Radiated power [kW]	221.6	219.5
Emittance [pm]	98 \rightarrow 126	5630
Energy spread [$\cdot 10^{-3}$]	1.03 \rightarrow 1.07	0.86

The injection makes use of a novel ‘anti-septum’ scheme based on an orbit bump formed by three dipole kickers. A current sheet is placed inside the middle kicker, which compensates the main field at the location where the injected beam passes [3]. The pulse of a kicker is weaker and shorter than in a septum magnet allowing the anti-septum to be as thin as 1 mm, reducing the distance between stored and injected beam and, therefore, the aperture requirements.

MAGNETS

Small apertures are a basic feature of low-emittance multi bend achromat lattices, because they enable an increase of magnet gradients and thus a reduction of magnet length and miniaturization of lattice cells. Many small magnets, in turn, result in small peak dispersion, such that sufficient momentum acceptance is still provided with small apertures. Due to miniaturization, the SLS 2.0 lattices contains 900 magnets in a 290.4 m circumference (of which 66 m are straights sections), which results in small inter-magnet distances and high fields and gradients.

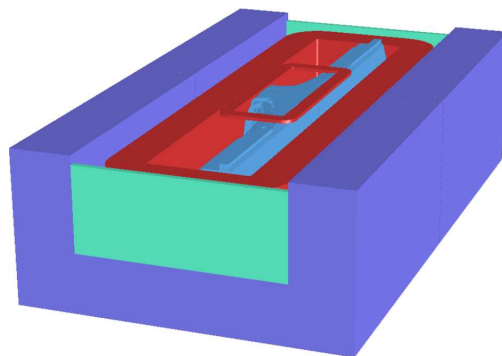


Figure 3: Resistive coil design for a central LGB with two vertical focusing combined function bends.

Content from this work may be used under the terms of the CC BY 3.0 licence (© 2018). Any distribution of this work must maintain attribution to the author(s), title of the work, publisher, and DOI.

The core component is a compound magnet containing the central LGB with about 2-T peak field, and two vertically focusing combined-function bending magnets (VB) in a common yoke. The RBs are essentially radially shifted quadrupoles. Resistive coil and permanent-magnet designs are being evaluated in parallel for the RB and the LGB compound magnet, the final decision depending on costs and ongoing technological progress in the field. Modified versions of these magnets are used in the dispersion suppressor cells at the ends of the arcs, i.e., half-LGBs and RBs and VBs with modified gradients. Designs using resistive coils (Fig. 3) as well as permanent magnet materials (Fig. 4) are under investigation. Given the advantages, the permanent magnet version is strongly preferred and we are preparing to build a LGB/VB prototype using these materials.

Any of the 60 LGBs may be exchanged by a LG-superbend; it is planned to start with three of these. The design is based on two pairs of coils, Nb₃Sn racetrack-coils to create a narrow central field peak of 6 Tesla, and NbTi Helmholtz coils to provide the required field integral [2].

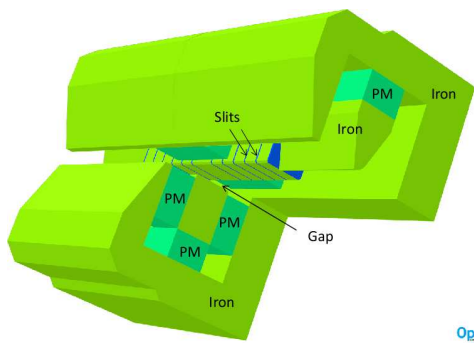


Figure 4: Three quarter model of central LGB with two vertical focusing combined function bends using permanent magnet material.

Quadruplets of quadrupoles on both ends of the arcs are used for matching to the straight sections and provide margin to compensate any focusing from the insertion device.

A total of 288 sextupoles and 144 octupoles are employed for correction of chromaticity and optimization of acceptance. Orbit control is performed using 120 horizontal and vertical dipoles realized with additional coils as integral part of some sextupoles and 24 small dipoles in the straight sections will be used to steer the photon beams from the undulators. Small quadrupoles for fine tuning and gradient corrections, and skew quadrupoles for coupling control, are realized with additional coils in some of the octupoles.

VACUUM

The vacuum chamber is based on a round beam pipe of 20-mm diameter. Sections with ante-chambers in the LGB regions, where radiation is emitted at high power, alternate with sections made from simple round pipes in the RB regions. Due to the high power density, the synchrotron radiation coming from the LGBs requires discrete crotch absorbers, otherwise distributed absorbers are used. The high

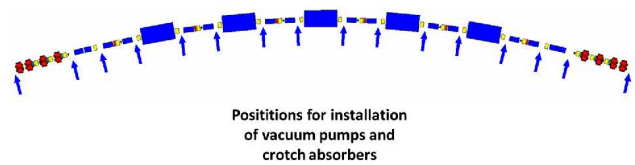


Figure 5: Magnet section with locations for vacuum pumps and crotch absorbers.

gas load originating at the crotch absorbers is evacuated in situ with local pumps (Fig. 5 shows the placement of pumps and absorbers). Vacuum conductance along the small diameter chamber is very low, therefore the vacuum chamber will be coated with non-evaporable getter (NEG) material for distributed pumping and to reduce radiation-induced gas desorption from the chamber walls. The NEG layer has a thickness of 1 μm in the ante-chambers but only 500 nm in the beam pipe in order to minimize the resistive wall effects.

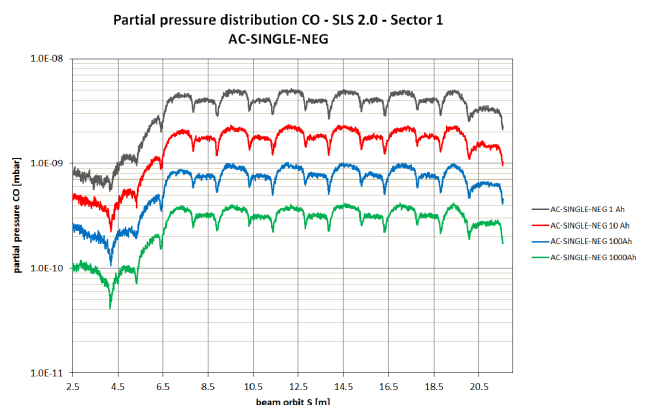


Figure 6: Pressure distributions for vacuum chamber with ante-chamber and NEG coating.

With Molflow+ [4] and Synrad+, the evolution of the pressure distribution inside the vacuum chamber with the ante-chamber was simulated for increasing beam doses (Fig. 6). A dose of 100 Ah should be sufficient to get below the required pressure of 10⁻⁹ mbar.

STABILITY

At the SLS, we have seen coupled bunch modes (CBM) in the longitudinal plane driven by higher order modes in the main RF cavities. In standard operation, suitable HOM tuning combined with Landau damping provided by a superconducting third harmonic cavity [5] is sufficient to control them. During filling of the ring, there are regions of instability, which require the longitudinal bunch by bunch feedback to be active. The upgrade will essentially use the same RF systems and the situation should be similar. An upgraded multi bunch feedback system with enhanced resolution and processing should even give a higher robustness. Transversally, we expect CBMs driven by resistive wakes and ions, these will be controlled by transverse feedbacks and the fill pattern gap.

Ion trapping can cause several adverse effects of beam performance as e.g. coherent instabilities, beam blow up, tune shift and increased coupling. The effect is reduced for the small beam sizes, we expect in SLS 2.0 and, if a gap of empty buckets is introduced in the regular bunch pattern. A detailed study was performed [6]. It shows that already a gap of 10 empty buckets will clean most of the ions inside the machine.

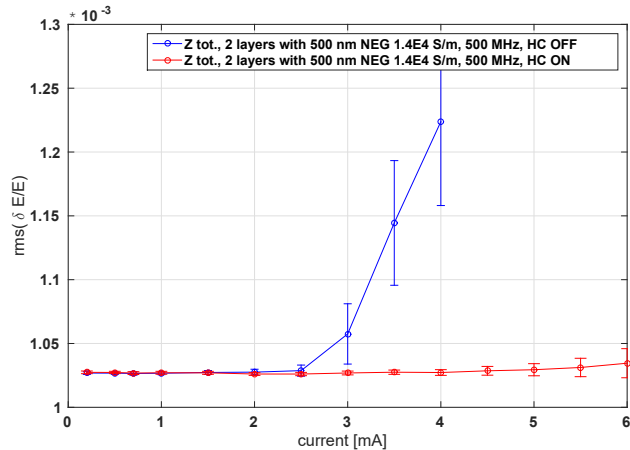


Figure 7: Single bunch energy spread versus bunch current as simulated with *mbtrack* (red: harmonic cavity on, blue, harmonic cavity off). The corresponding thresholds for the microwave instability are 1.5, resp. 3.5 mA.

The onset of turbulent bunch lengthening has been estimated using *mbtrack* [7]. The simulations (Fig. 7) include impedance contributions from vacuum chamber, beam-position monitors, tapers and cavities, the onset of the instability shows up as an increase of the single bunch energy spread with current. The resulting threshold current of 1.5 mA without, and 3.5 mA with an ideal third-harmonic RF system for bunch lengthening, is well above the desired beam current of about 1 mA per bunch (400 mA total current). CSR limits are of a similar order.

NEXT STEPS

The year 2017 saw the end of the conceptional phase of the upgrade with a review of the conceptional design report. Currently, we enter the technical design phase, which should be concluded in summer 2019. The beamlines, which partially require to be adapted to the new machine layout also go through conceptional and technical design phases until mid 2021. In 2023/2024, SLS will enter a 18 month long ‘dark time’ (without any user operation), during which the shielding will be modified, the storage ring and the undulators will be replaced and accelerator and beamlines will be commissioned.

The authors acknowledge the contribution of all team members of the SLS 2.0 project team.

REFERENCES

- [1] A. Streun (Ed.), “SLS-2 Conceptual Design Report”, PSI-Bericht 17-03, Paul Scherrer Institut, Villigen, Switzerland, Dec. 2017.
- [2] C. Calzolaio et al., “Design of a Superconducting Longitudinal Gradient Bend Magnet for the SLS Upgrade”, IEEE Trans. Applied Supercon., vol. 27, no. 4, 2017.
- [3] C. Gough, M. Aiba, “Top-up injection with anti-septum”, Proc. IPAC 2017, Copenhagen, Denmark, pp. 774-776, 2017
- [4] M. Ady, R. Kersevan and M. Grabski, “Monte Carlo simulations of synchrotron radiation and vacuum performance of the MAX IV light source”, Proc. IPAC-2014, Dresden, Germany (2014).
- [5] M. Svandrlík et al., “The super-3HC project: An idle superconducting harmonic cavity for bunch length manipulation”, Proc. EPAC-2000, Vienna, Austria (2000).
- [6] A. Wrulich, “Ion trapping in SLS-2”, Technical report SLS2-WA80_001. PSI, 2017
- [7] G. Skripka et al., “Simultaneous computation of intrabunch and interbunch collective beam motions in storage rings”, Nucl. Instr. and Meth. A 806, 221-230, 2016.